

## Analysis of air-to-water converter frame using ANSYS simulation

Naufal Waliy Ishlah\*, Salvatore Johannes Rega, Triwahyudin Rohman, Subekti Subekti

\* Department of Mechanical Engineering, Faculty of Engineering, Mercu Buana University, Jakarta, Indonesia Jln. Raya Meruya Selatan No.1 West Jakarta, Indonesia DKI Jakarta

\*✉ [naufalwaliy45@gmail.com](mailto:naufalwaliy45@gmail.com)

Submitted: 05/04/2024

Revised: 31/05/2024

Accepted: 08/06/2024

**Abstract:** According to projections made by the Indonesian Institute of Sciences (LIPI), by 2040 every region along Java's northern coast—from Banten to Surabaya and Iswara—will be an urban area vulnerable to water scarcity. As a result, more careful consideration is required. Since air is an endless supply, turning it into water is one way to address the clean water shortage. A good design's structure is one of its essential components. This is because the device's structure must sustain both the renewable energy source and the complete system. By utilizing ANSYS Workbench and theoretical calculations to analyze the maximum stress results, the research aims to ascertain whether the machine frame is safe for usage. In this investigation, the ANSYS 2021 R1 software was used to apply the finite element method to ASTM A36 material under vertical loading. The air-to-water converter mechanism is still safe after simulations were run on its shaft and frame. This is demonstrated by the biggest maximum stress on the shaft (6.2194 MPa) from the ANSYS numerical simulation and the largest maximum stress (0.349 MPa) on the frame, both of which are still below the allowable stress. Furthermore, a 0.9694 difference in safety factor was found between theoretical calculations and shaft simulation, and a 0.1573 difference was found for the frame. The safety factor acquired from the shaft was 1.6043, while the safety factor gained from the frame was 1.6073.

**Keywords:** Simulation; frame; finite element; ANSYS.

### 1. INTRODUCTION

According to the Indonesian Institute of Sciences (LIPI), by 2040, all of Java's northern coastal regions—from Banten to Surabaya and Iswara—will be urbanized and vulnerable to water scarcity. As a result, more careful consideration is required. Because air is an endless supply, turning it into water is one way to address the clean water shortage [1][2]. The structure of a good design is one of the things that must be done. This is because the device's structure must sustain both the renewable energy source and the complete system [3].

The frame is the most crucial part, particularly in machinery, because it supports the other parts and keeps the machine stable by preventing moment, axial, and normal forces [4][5]. Typically, frames are composed of metal or composite materials to guarantee their strength and ability to support loads while preserving the rigidity of the structure [6][7].

Owing to its crucial function, it is imperative to examine the potential peak stresses within the frame [8][9]. With this procedure, a thorough examination of the frame design is carried out using ANSYS software [10][11]. ANSYS is a software that relies on Finite Element Analysis (FEA) and is designed to help solve mechanical problems [12][13]. Static/dynamic, linear and nonlinear structural analysis, heat transfer, fluid problems, and electromagnetic concerns are some of these issues [14][15].

At Singaperbangsa University Karawang, mechanical engineering majors have studied the simulation of safety factors and frame loads. Furthermore, several designs for waste processing equipment have been conducted by Mercu Buana University students. Meanwhile, the creation of turbines inside pipelines has sparked research into renewable energy.

The purpose of this study is to validate theoretical calculations with analytical results using ANSYS Workbench software and to ascertain the safety of the machine frame by assessing the maximum stress values using both theoretical approaches and ANSYS Workbench.

### 2. METHOD



JTTM: Jurnal Terapan Teknik Mesin is licensed under a Creative Commons Attribution-NonCommercial 4.0 International License.

The first step in this research was to conduct a literature review of earlier studies that were pertinent to the research topic. Then, data was gathered, and the frame analysis was completed. Simulation procedures included designing, characterizing element kinds and material characteristics, applying loads to the structure in the form of component weights supported by the frame, evaluating simulation results, and validating theoretical calculations with ANSYS. Specifics are displayed in Figure 1.

Figure 1 shows how the research is conducted. To identify cause-and-effect phenomena in design, this study used an experimental approach that combined the finite element method with static-free simulation. The aluminum alloy 6061 pipe used in the investigation had an inner diameter of 21 mm and an outside diameter of 26 mm at the top and 23 mm at the bottom, simulating a shaft. Furthermore, ASTM A36 material with hollow iron dimensions of 30 mm x 30 mm x 2 mm and angle iron dimensions of 40 mm x 40 mm x 3 mm was used in the frame simulation. Figure 2 shows each component's design for a better understanding. The material qualities utilized in the study are displayed in Figure 1.

Table 1. ASTM A36 material properties.

No.	Properties	Value
1	Density	7.85 g/cm <sup>3</sup>
2	Young's Modulus	200 GPa
2	Tensile Strength, Ultimate	400 MPa
3	Yield Strength	250 MPa
4	Bulk Modulus	138,89 GPa
5	Shear Modulus	79,3 GPa

Table 2. Aluminum alloy 6061 material properties.

No.	Properties	Nilai
1	Density	2.7 g/cm <sup>3</sup>
2	Young modulus	69 GPa
3	Tensile Strength, Ultimate	310 MPa
4	Yield Strength	276 MPa
5	Bulk Modulus	67.647 GPa
6	Shear Modulus	25.94 GPa

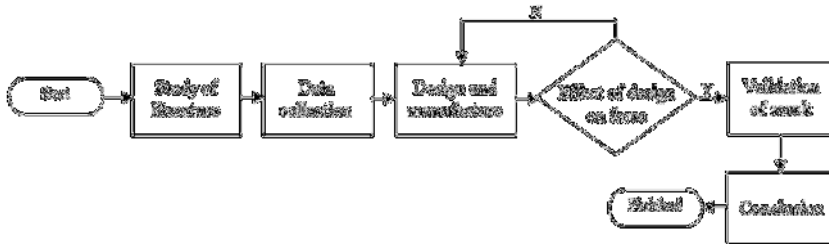


Figure 1. Research flowchart.

The frame's design—which includes the shaft and the frame—that will be subjected to static load simulation is shown below. According to Figure 2.

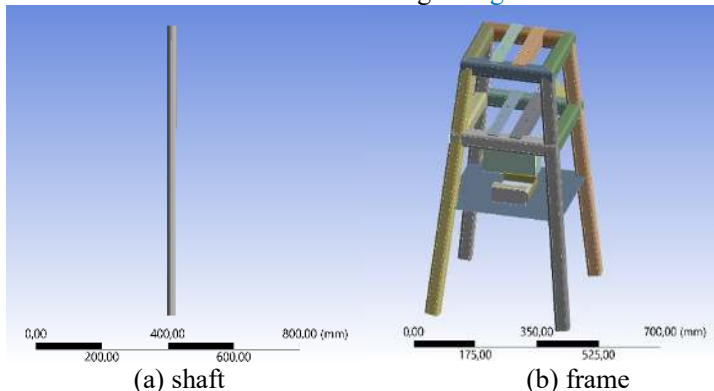


Figure 2. Shaft geometry design (a) and frame (b) design.

Next, by dividing the material's yield strength by the stress value derived from the simulation, the validation of the safety factor of the shaft and frame designs may be computed. To provide clarity, you can use the following equation:

$$sf = \frac{\text{yield stress}}{\text{Calculate stress}} \quad (1)$$

### 3. RESULTS AND DISCUSSION

#### Equivalent von Mises stress analysis

The static stress analysis simulation results are displayed in [Error! Reference source not found.](#) (a) and (b) for the frame design with a 24 N load applied to the angle iron and for the shaft design with an 8 N load at the center of the pipe and 33.32 N at the bottom. The load on each of the frame's four legs is causing reaction forces of 12.05 N.

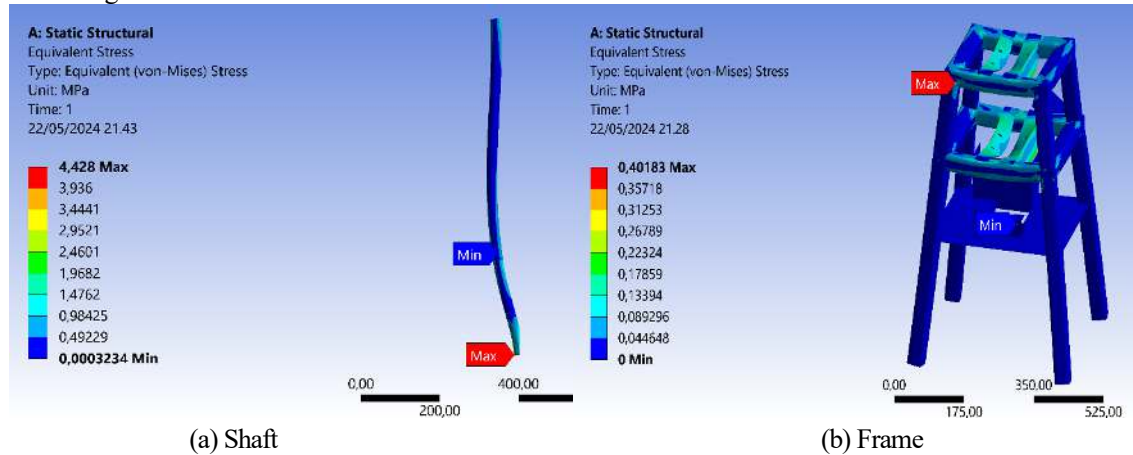


Figure 3. The equivalent von Mises stress values for (a) the shaft design and (b) the frame design.

The von Mises stress is 0.40183 MPa for the frame and 4.428 MPa for the shaft. The material's yield strength is still exceeded by both von Mises stresses. The yield strength value should be less than the analysis results (Von-Mises stress).

#### Analisis total deformasi

The simulation results of the overall deformation of the shaft and frame design are displayed in [Figure 4](#) (a) and (b). The frame is deformed by 0.00114 mm, whereas the shaft deforms by 0.046 mm.

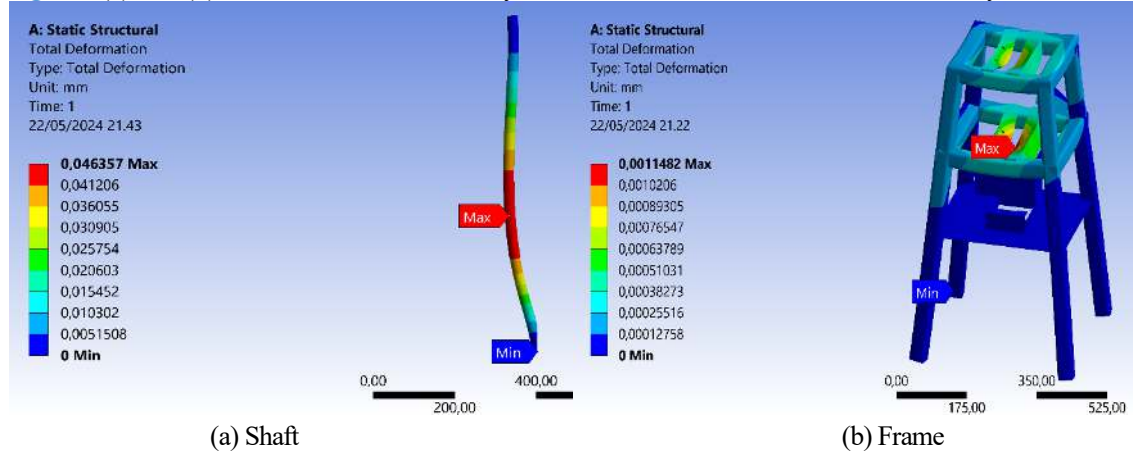


Figure 4. Total deformation of the (a) shaft design and (b) frame design.

The center region of the shaft pipe, designated in red, is where the maximum overall deformation in the frame simulation results is 0.046 mm, as seen in [Figure 4](#). The final support point for the parts supporting the blade and shaft load is the bottom center of the angle iron, where the maximum total

deformation in the frame simulation results displayed in Figure 4 is 0.00114 mm. Considering that the stress is less than the material's yield strength, both deformation outcomes are still in the minor category.

Maximum stress analysis

The maximum stress simulation results for the shaft and frame designs are displayed in Figure 5(a) and (b). The shaft's maximum stress is 6.2194 MPa, whereas the frame's maximum stress is 0.349 MPa

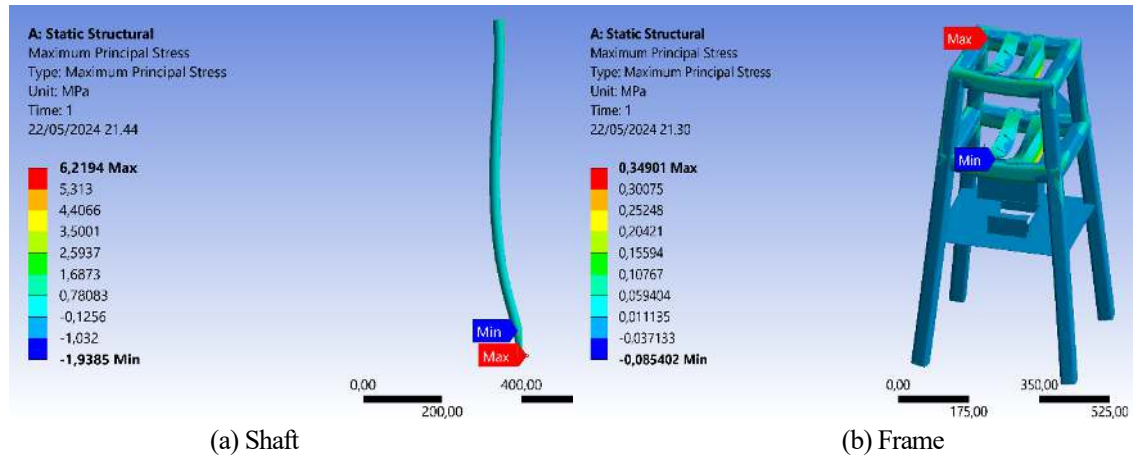


Figure 5. Maximum stress values for (a) shaft design and (b) frame design.

In the shaft simulation results displayed in Figure 5, the lowest point of the shaft exhibits a maximum stress of 6.2194 MPa. Similarly, the connection point on the frame is where the greatest stress of 0.349 MPa is found in the frame. The result obtained shows that there will be no plastic (permanent) deformation of the structure because it is much below the yield strength limit [16].

Safety factor analysis

The surface reaction in the safety factor simulation for the shaft and frame designs is depicted in Figure 6. (a) and (b). The safety factor values derived for the shaft and frame should be less than two to achieve a good safety factor under static loads.

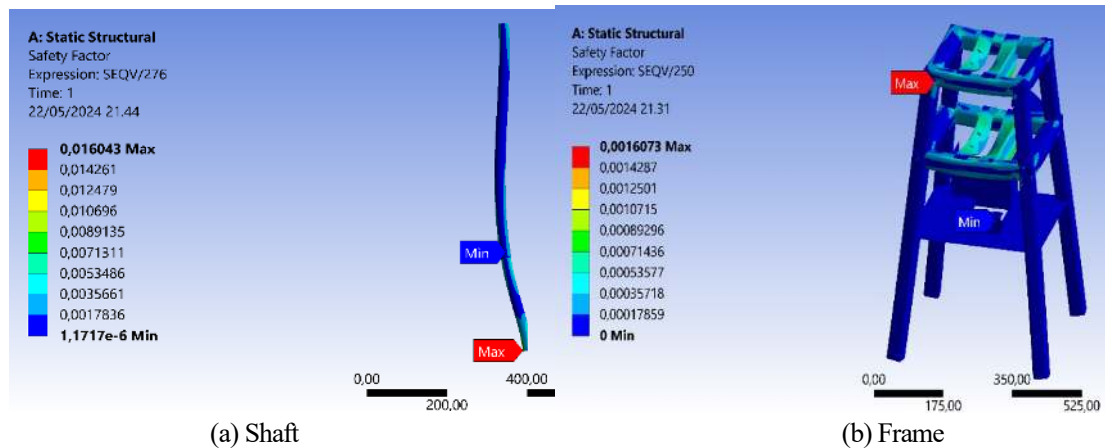


Figure 6. Safety factor results for (a) shaft design and (b) frame design.

The blue to green color range represents the safety factor result for the shaft design, which is 1.6043. This indicates that the shaft is both efficient and safe to operate. Since the safety factor is less than 2, using it is safe up to this point. Redesigning is not essential because the safety factor value of 1.6043 is already very good for static loading and efficiency. The frame design's safety factor is 1.6073. The blue-to-green color spectrum denotes this, indicating that the construction is well-efficient and safe to utilize.

Because the safety factor obtained is less than 2, it can be used safely. The redesign is not essential because a safety factor value of 1.6073 is already very good for static loading and efficiency.

Validation of theoretical and ansys safety factor calculation

The percentage discrepancy between the computer computational results and the calculation results using formulas specific to each design is ascertained through design validation. The data of analytical calculation outcomes employing formulas are shown below:

a. Shaft Design

$$sf = \frac{\text{yield stress}}{\text{Calculate stress}}$$

$$sf = \frac{276}{1.07235}$$

$$sf = 2.5737$$

b. Frame Design

$$sf = \frac{\text{yield stress}}{\text{Calculate stress}}$$

$$sf = \frac{250}{1.72414}$$

$$sf = 1.45$$

Clearer understanding, refer to [Table 3](#), for the difference in safety factors between the computer calculation results and the analytical calculation using formulas:

**Table 3.** Validation of safety factors for shaft and frame designs

No	Frame Part	Theoretical Calculation Result	ANSYS Workbench Simulation Result	Calculation Difference
1	Shaft	2.5737	1.6043	0.9694
2	Frame	1.45	1.6073	0.1573

The air-to-water converter system's shaft and frame will be validated to verify the simulation results using hand calculations. The theoretical calculations for the shaft and the simulation results provide a discrepancy of 0.9694. The theoretical calculations for the frame and the simulation results provide a discrepancy of 0.1636. This is because the discretization division may have an impact on the outcomes of the simulation. According to [Table 3](#).

### 3 CONCLUSION

Inferences can be made from the results acquired from numerical analysis utilizing ANSYS Workbench 21.1 and theoretical calculations. Specifically, as can be seen from the maximum stress since the loads are still below the allowable stress of the frame material, the structure of the air-to-water converter frame is safe even after being subjected to loads like forces operating on the tool. Maximum stress of 6.2194 MPa, total deformation of 0.046 mm, Von Mises stress of 4.428 MPa, and safety factor of 1.6043 are displayed in the simulation results for the shaft design conducted using Ansys. The Von Mises stress is 0.40183 MPa, the safety factor is 1.6073, the maximum stress obtained is 0.349 MPa, and the total deformation is 0.00114 mm for the frame design. The frame shows that the component satisfies safety requirements both theoretically and through simulation, while analysis of the shaft shows that the Ansys simulation yields a superior safety factor than the analytical calculations using formulas.

### REFERENCE

[1] W. Xu and O. M. Yaghi, "Metal-Organic Frameworks for Water Harvesting from Air, Anywhere, Anytime," *ACS Cent. Sci.*, vol. 6, no. 8, pp. 1348–1354, 2020, doi: 10.1021/acscentsci.0c00678.

- [2] E. Ahmadi, B. McLellan, B. Mohammadi-Ivatloo, and T. Tezuka, "The role of renewable energy resources in sustainability of water desalination as a potential fresh-water source: An updated review," *Sustain.*, vol. 12, no. 13, 2020, doi: 10.3390/su12135233.
- [3] B. A. Rayan, U. Subramaniam, and S. Balamurugan, "Wireless Power Transfer in Electric Vehicles: A Review on Compensation Topologies, Coil Structures, and Safety Aspects," *Energies*, vol. 16, no. 7, 2023, doi: 10.3390/en16073084.
- [4] M. Rizki, A. Gamayel, and M. Zaenudin, "Simulation on the influence of the shape of the carabiner as a hanging accessory on stress distribution using Autodesk Fusion 360," *JTTM J. Terap. Tek. Mesin*, vol. 5, no. 1, pp. 33–40, 2024, doi: 10.37373/jttm.v5i1.779.
- [5] P. A. Arrabiyeh, D. May, M. Eckrich, and A. M. Dlugaj, "An overview on current manufacturing technologies: Processing continuous rovings impregnated with thermoset resin," *Polym. Compos.*, vol. 42, no. 11, pp. 5630–5655, 2021, doi: 10.1002/pc.26274.
- [6] M. Mohammadi, M. A. Kafi, A. Kheyroddin, and H. R. Ronagh, "Performance of innovative composite buckling-restrained fuse for concentrically braced frames under cyclic loading," *Steel Compos. Struct.*, vol. 36, no. 2, pp. 163–177, 2020, doi: 10.12989/scs.2020.36.2.163.
- [7] T. Pravilonis and E. Sokolovskij, "Analysis of composite material properties and their possibilities to use them in bus frame construction," *Transport*, vol. 35, no. 4, pp. 368–378, 2020, doi: 10.3846/transport.2020.13018.
- [8] R. M. Marchin, D. Backes, A. Ossola, M. R. Leishman, M. G. Tjoelker, and D. S. Ellsworth, "Extreme heat increases stomatal conductance and drought-induced mortality risk in vulnerable plant species," *Glob. Chang. Biol.*, vol. 28, no. 3, pp. 1133–1146, 2022, doi: 10.1111/gcb.15976.
- [9] C. Grossiord *et al.*, "Plant responses to rising vapor pressure deficit," *New Phytol.*, vol. 226, no. 6, pp. 1550–1566, 2020, doi: 10.1111/nph.16485.
- [10] A. A. Shittu, A. Mehmanparast, P. Hart, and A. Kolios, "Comparative study between S-N and fracture mechanics approach on reliability assessment of offshore wind turbine jacket foundations," *Reliab. Eng. Syst. Saf.*, vol. 215, 2021, doi: 10.1016/j.res.2021.107838.
- [11] A. Agarwal and L. Mthembu, "Structural Analysis and Optimization of Heavy Vehicle Chassis Using Aluminium P100/6061 Al and Al GA 7-230 MMC," *Processes*, vol. 10, no. 2, 2022, doi: 10.3390/pr10020320.
- [12] M. Alhijazi, Q. Zeeshan, Z. Qin, B. Safaei, and M. Asmael, "Finite Element Analysis of Natural Fibers Composites: A Review," *Nanotechnol. Rev.*, vol. 9, no. 1, pp. 853–875, 2020, doi: 10.1515/ntrev-2020-0069.
- [13] A. B. Kakarla, I. Kong, S. G. Nukala, and W. Kong, "Mechanical Behaviour Evaluation of Porous Scaffold for Tissue-Engineering Applications Using Finite Element Analysis," *J. Compos. Sci.*, vol. 6, no. 2, pp. 1–10, 2022, doi: 10.3390/jcs6020046.
- [14] D. V. Alexandrov and A. Y. Zubarev, "Patterns in soft and biological matters," *Philos. Trans. R. Soc. A Math. Phys. Eng. Sci.*, vol. 378, no. 2171, 2020, doi: 10.1098/rsta.2020.0002.
- [15] A. Krishna, "A Review on Vibro-Acoustic Analysis of a Launch Vehicle Structure," *Int. J. Res. Appl. Sci. Eng. Technol.*, vol. 10, no. 6, pp. 4154–4157, 2022, doi: 10.22214/ijraset.2022.44873.
- [16] R. K. Abu Al-Rub, D.-W. Lee, K. A. Khan, and A. N. Palazotto, "Effective Anisotropic Elastic and Plastic Yield Properties of Periodic Foams Derived from Triply Periodic Schoen's I-WP Minimal Surface," *J. Eng. Mech.*, vol. 146, no. 5, 2020, doi: 10.1061/(asce)em.1943-7889.0001759.